Numerical approximation of flow in a symmetric channel with vibrating walls

P. Sváček^{a,b,*}, J. Horáček^{a}

^{a}*Institute of Thermomechanics, Czech Academy of Sciences, Dolejškova 5, 182 00 Praha 8, Czech Republic*

^{b}*Dep. of Technical Mathematics, Faculty of Mechanical Engineering, Czech Technical University in Prague, Karlovo nam. 13, 121 35 Praha 2, Czech Republic*

Abstract

In this paper the numerical solution of two dimensional fluid-structure interaction problem is addressed. The fluid motion is modelled by the incompressible unsteady Navier-Stokes equations. The spatial discretization by stabilized finite element method is used. The motion of the computational domain is treated with the aid of Arbitrary Lagrangian Eulerian (ALE) method. The time-space problem is solved with the aid of multigrid method.

The method is applied onto a problem of interaction of channel flow with moving walls, which models the air flow in the glottal region of the human vocal tract. The pressure boundary conditions and the effects of the isotropic and anisotropic mesh refinement are discussed. The numerical results are presented.

© 2010 University of West Bohemia. All rights reserved.

1. Introduction

This paper is concerned with numerical simulation of unsteady viscous incompressible flow in a simplified model of the glottal region of the human vocal tract with the aid of the finite element method (FEM). The main attention is paid to the efficient computation of the flow field. For the robust and efficient solver both the advanced stabilization (as streamline upwind/Petrov Galerkin stabilizations, cf. [6, 7]) and solution methods (as multigrid and/or domain decomposition, cf. [19, 9, 10, 13]) have to be employed.

FEM is well known as a general discretization method for partial differential equations. It can handle easily complex geometries and also boundary conditions employing derivatives. However, straightforward application of FEM procedures often fails in the case of incompressible Navier-Stokes equations. The reason is that momentum equations are of advection-diffusion type with dominating advection. The Galerkin FEM leads to unphysical solutions if the grid is not fine enough in regions of strong gradients (e.g. boundary layer). In order to obtain physically admissible correct solutions it is necessary to apply suitable mesh refinement (e.g. anisotropically refine mesh, cf. [5]) combined with a stabilization technique, cf. [7, 3, 18, 16].

Furthermore, the time and space discretized linearized problem of the arising large system of linear equations needs to be solved in fast and efficient manner. The application of direct solvers as UMFPACK (cf. [4]) leads to robust method, where different stabilizations procedures can be easily applied even on anisotropically refined grids. However, the application of direct solver

---

*Corresponding author. Tel.: +420 224 357 413, e-mail: Petr.Svacek@fs.cvut.cz.

for system of equations with more than approximately 10^5 unknowns becomes unfeasible in many cases (depending on computer CPU and memory).

In that case the application of multigrid (cf. [19]) or domain decomposition methods is an option, cf. [13]. In this paper a simplified version of multigrid method is shortly described together with a choice of finite elements and stabilization procedures. Even when the method is simplified, it was found to be efficient and robust enough.

The developed method is applied to the numerical solution of a channel flow modelling the glottal region of the human vocal tract including the vibrating vocal fold. The vibrations of the channel wall are prescribed, see [14]. Further, in order to obtain physically relevant results the pressure drop boundary conditions are employed, cf. [8].

First, the mathematical model consisting of time dependent computational domain and incompressible flow model is introduced. Further, in Section 3 the time and space discretization is described and Section 4 describes the application of a simple multigrid version. Section 5 shows the numerical results.

2. Mathematical model

The model problem consists of flow model, which describes the fluid motion in the time-dependent computational domain Ω_t, i.e. in a channel with moving walls, see Fig. 1. For the description and the approximation on moving meshes the Arbitrary Lagrangian-Eulerian (ALE) method is employed, cf. [12]. The geometry of the channel is chosen according [14], where a different distance between the moving walls, i.e. the gap $g(t)$, was considered. Further, on the outlet part of the channel a modification of do-nothing boundary condition was applied in order to allow the vortices flow smoothly out of the computational domain. On the inlet either the Dirichlet boundary condition for velocity is prescribed or preferably we use the pressure drop formulation, similarly as in cf. [8]. The presented mathematical model (and also its numerical approximation) is a slight modification of the mathematical model applied to the numerical simulation of flow induced airfoil vibrations in our previous works, cf. [18].

2.1. Arbitrary Lagrangian Eulerian method

In order to treat the fluid flow on moving domains, the so-called Arbitrary Lagrangian Eulerian method is used. We assume that $\mathcal{A} = \mathcal{A}(\xi, t) = \mathcal{A}_t(\xi)$ is an ALE mapping defined for all
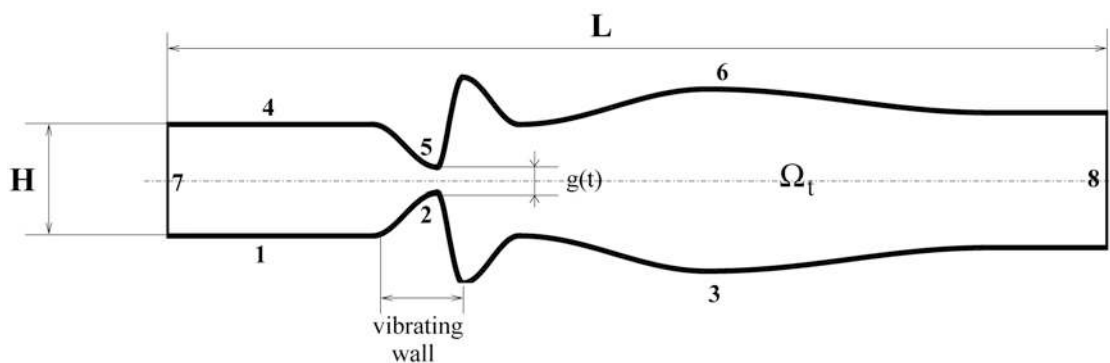

Fig. 1. Computational domain and boundary parts: The inlet part of the boundary Γ_I (number 7), the outlet part of the boundary Γ_O (number 8), the fixed walls Γ_D (numbers 1,4,3,6) and vibrating walls Γ_{Wt} (numbers 2, 5)

$t \in (0, T)$ and $\xi \in \Omega_0$, which is smooth enough and continuously differentiable mapping of $\xi \in \Omega_0$ onto $x \in \Omega_t$, $x = \mathcal{A}_t(\xi)$. We define the *domain velocity* $\mathbf{w}_D : \mathcal{M} \to \mathbb{R}$ satisfies

$$\mathbf{w}_D(x, t) = \frac{\partial \mathcal{A}}{\partial t}(\xi, t) \qquad \text{for all } \xi \in \Omega_0 \text{ and } t \in (0, T), \quad \text{where } x = \mathcal{A}(\xi, t). \tag{1}$$

Furthermore the symbol $D^{\mathcal{A}}/Dt$ denotes the ALE derivative, i.e. the time derivative with respect to the reference configuration. The ALE derivative satisfies (cf. [18, 11])

$$\frac{D^{\mathcal{A}} f}{Dt}(x, t) = \frac{\partial f}{\partial t}(x, t) + \mathbf{w}_D(x, t) \cdot \nabla f(x, t). \tag{2}$$

In the present paper the ALE mapping is analytically prescribed, but in the future this mapping will be a part of the solution similarly as in cf. [18].

2.2. Flow model

Let us consider the following system of the incompressible Navier-Stokes equations in a bounded time-dependent domain $\Omega_t \subset R^2$ written in ALE form

$$\frac{D^{\mathcal{A}} \mathbf{v}}{Dt} - \nu \triangle \mathbf{v} + ((\mathbf{v} - \mathbf{w}_D) \cdot \nabla) \mathbf{v} + \nabla p = 0, \qquad \nabla \cdot \mathbf{v} = 0, \qquad \text{in } \Omega_t, \tag{3}$$

where $\mathbf{v} = \mathbf{v}(x, t)$ is the flow velocity, $p = p(x, t)$ is the kinematic pressure (i.e. pressure divided by the constant fluid density ρ_∞) and ν is the kinematic viscosity.

The boundary of the computational domain $\partial \Omega_t$ consists of mutually disjoint parts Γ_D (wall), Γ_I (inlet), Γ_O (outlet) and the moving part Γ_{Wt} (oscillating wall). The following boundary conditions are prescribed

$$
\begin{aligned}
&\text{a)} \quad \mathbf{v}(x, t) = \mathbf{0} && \text{for } x \in \Gamma_D, \\
&\text{b)} \quad \mathbf{v}(x, t) = \mathbf{w}_D(x, t) && \text{for } x \in \Gamma_{Wt}, \\
&\text{c)} \quad -(p - p_{ref}^o)\mathbf{n} + \tfrac{1}{2}(\mathbf{v} \cdot \mathbf{n})^- \mathbf{v} + \nu \frac{\partial \mathbf{v}}{\partial \mathbf{n}} = 0, && \text{on } \Gamma_O, \\
&\text{d)} \quad -(p - p_{ref}^i)\mathbf{n} + \tfrac{1}{2}(\mathbf{v} \cdot \mathbf{n})^- \mathbf{v} + \nu \frac{\partial \mathbf{v}}{\partial \mathbf{n}} = 0, && \text{on } \Gamma_I,
\end{aligned}
\tag{4}
$$

where $\mathbf{n}$ denotes the unit outward normal vector, the constants p_{ref}^i, p_{ref}^o denotes the reference pressure values, and α^- denotes the negative part of a real number α. In computations the condition (4d) can be replaced by the condition

$$\text{e)} \quad \mathbf{v}(x, t) = \mathbf{v}_D \qquad \text{for } x \in \Gamma_I. \tag{5}$$

Finally, we prescribe the initial condition

$$\mathbf{v}(x, 0) = \mathbf{v}^0(x) \qquad \text{for } x \in \Omega_0.$$

3. Numerical approximation

In this section the numerical approximation of the mathematical model given in Section 2 is shown. As already mentioned the presented numerical approximation is a slight modification of our previous works, cf. [18, 17]. Nevertheless there are several significant differences, which were found to be important for the numerical approximation: boundary conditions used on the inlet/outlet part of the computational domain and their weak formulation, a modified Galerkin/Least-Squares (GLS) scheme employed for stable pair of finite elements, and the choice of stabilizing parameters. The space discretization and its stabilization is briefly desribed for the sake of clarity and completeness.

3.1. Time discretization

We consider a partition $0 = t_0 < t_1 < \ldots < T$, $t_k = k\Delta t$, with a time step $\Delta t > 0$, of the time interval $(0, T)$ and approximate the solution $\mathbf{v}(\cdot, t_n)$ and $p(\cdot, t_n)$ (defined in Ω_{t_n}) at time t_n by $\mathbf{v}^n$ and p^n, respectively. For the time discretization we employ a second-order two-step scheme using the computed approximate solution $\mathbf{v}^{n-1}$ in $\Omega_{t_{n-1}}$ and $\mathbf{v}^n$ in Ω_{t_n} for the calculation of $\mathbf{v}^{n+1}$ in the domain $\Omega_{t_{n+1}} = \Omega_{n+1}$. We write

$$\frac{\partial \mathbf{v}}{\partial t}(x, t^{n+1}) \approx \frac{3\mathbf{v}^{n+1} - 4\hat{\mathbf{v}}^n + \hat{\mathbf{v}}^{n-1}}{2\Delta t} \qquad \text{where } x \in \Omega_{n+1}, \tag{6}$$

where $\hat{\mathbf{v}}^n$ and $\hat{\mathbf{v}}^{n-1}$ are the approximate solutions $\mathbf{v}^n$ and $\mathbf{v}^{n-1}$ defined on Ω_n and Ω_{n-1}, respectively, and transformed onto Ω_{n+1} with the aid of ALE mapping, i.e. $\hat{\mathbf{v}}^i(x) = \mathbf{v}^i(\mathcal{A}_{t_i}(\xi))$ where $x = \mathcal{A}_{t_{n+1}}(\xi) \in \Omega_{n+1}$. Further, we approximate the domain velocity $\mathbf{w}_D(x, t_{n+1})$ by $\mathbf{w}_D{}^{n+1}$, where

$$\mathbf{w}_D{}^{n+1}(x) = \frac{3\mathcal{A}_{t_{n+1}}(\xi) - 4\mathcal{A}_{t_n}(\xi) + \mathcal{A}_{t_{n-1}}(\xi)}{2\Delta t}, \qquad x = \mathcal{A}_{t_{n+1}}(\xi), \ x \in \Omega_{n+1}.$$

Then the time discretization leads to the following problem in domain Ω_{n+1}

$$\frac{3\mathbf{v}^{n+1} - 4\hat{\mathbf{v}}^n + \hat{\mathbf{v}}^{n-1}}{2\Delta t} - \nu\triangle\mathbf{v}^{n+1} + \left((\mathbf{v}^{n+1} - \mathbf{w}_D{}^{n+1}) \cdot \nabla\right)\mathbf{v}^{n+1} + \nabla p^{n+1} = 0, \tag{7}$$

$$\nabla \cdot \mathbf{v}^{n+1} = 0,$$

equipped with boundary conditions (4a–d) and the initial condition.

3.2. Weak formulation

For solution of the problem by finite element method, the time-discretized problem (7) is reformulated in a weak sense. The following notation is used: By $W = \mathbf{H}^1(\Omega_{n+1})$ the velocity space is defined, by X the space of test functions is denoted

$$X = \{\mathbf{z} \in W : \mathbf{z} = 0 \text{ on } \Gamma_{Wt_{n+1}} \cup \Gamma_D\},$$

and by $Q = L^2(\Omega_{n+1})$ the pressure space is denoted. Using the standard approach, cf. [18], the solution $\mathbf{v} = \mathbf{v}^{n+1}$ and $p = p^{n+1}$ of problem (7) satisfies

$$a(U, V) = f(V), \qquad U = (\mathbf{v}, p) \tag{8}$$

for any $V = (\mathbf{z}, q) \in X \times Q$. Here, the forms $a(\cdot, \cdot)$ and $f(\cdot)$ are defined for any U, V by

$$a(U, V) = \left(\frac{3}{2\Delta t}\mathbf{v}, \mathbf{z}\right) + \nu\left(\nabla\mathbf{v}, \nabla\mathbf{z}\right) + \mathcal{B}(\mathbf{v}, \mathbf{z}) + c_n(\mathbf{v}; \mathbf{v}, \mathbf{z}) - (p, \nabla \cdot \mathbf{z}) + (\nabla \cdot \mathbf{v}, q),$$

$$f(V) = \frac{1}{2\Delta t}\left(4\hat{\mathbf{v}}^n - \hat{\mathbf{v}}^{n-1}, \mathbf{z}\right) - \int_{\Gamma_I} p_{ref}^i \mathbf{v} \cdot \mathbf{n} \, \mathrm{d}S - \int_{\Gamma_O} p_{ref}^o \mathbf{v} \cdot \mathbf{n} \, \mathrm{d}S,$$

and for any $\mathbf{w}, \mathbf{v}, \mathbf{z} \in W$

$$c_n(\mathbf{w}, \mathbf{v}, \mathbf{z}) = \int_{\Omega_{n+1}} \left(\frac{1}{2}(\mathbf{w} \cdot \nabla\mathbf{v}) \cdot \mathbf{z} - \frac{1}{2}(\mathbf{w} \cdot \nabla\mathbf{z}) \cdot \mathbf{v}\right) \mathrm{d}x - \left((\mathbf{w}_D{}^{n+1} \cdot \nabla)\mathbf{v}, \mathbf{z}\right),$$

$$\mathcal{B}(\mathbf{v}, \mathbf{z}) = \int_{\Gamma_I \cup \Gamma_O} \frac{1}{2}(\mathbf{v} \cdot \mathbf{n})^+ \mathbf{v} \cdot \mathbf{z} \, \mathrm{d}S,$$

where by $(\cdot, \cdot)$ we denote the scalar product in the space $L^2(\Omega_{n+1})$.

3.3. Spatial discretization

Further, the weak formulation (8) is approximated by the use of FEM: we restrict the couple of spaces (X, M) to finite element spaces (X_h, M_h). First, the computational domain Ω_t is assumed to be polygonal and approximated by an admissible triangulation $\mathcal{T}_h$, cf. [2]. Based on the triangulation $\mathcal{T}_h$ the Taylor-Hood finite elements are used, i.e.

$$
\begin{aligned}
\mathcal{H}_h &= \{v \in C(\overline{\Omega_{n+1}}); v|_K \in P_2(K) \text{ for each } K \in \mathcal{T}_h\}, \\
\mathcal{W}_h &= [\mathcal{H}_h]^2, \qquad X_h = \mathcal{W}_h \cap \mathcal{X}, \\
\mathcal{M}_h &= \{v \in C(\overline{\Omega_{n+1}}); v|_K \in P_1(K) \text{ for each } K \in \mathcal{T}_h\}.
\end{aligned}
\tag{9}
$$

The couple (X_h, M_h) satisfy the Babuška-Brezzi inf-sup condition, which guarantees the stability of a scheme, cf. [20].

Problem 1 (Galerkin approximations). *Find $U_h = (\mathbf{v}_h, p_h) \in (X_h, M_h)$ such that $\mathbf{v}_h$ satisfy boundary conditions (4a,b) and*

$$
a(U_h, V_h) = f(V_h),
\tag{10}
$$

for all $\mathbf{z}_h \in X_h$ and $q_h \in M_h$.

The Galerkin approximations are unstable in the case of high Reynolds numbers, when the convection dominates. In that case a stabilized method needs to be applied.

3.4. Stabilization

In order to overcome the above mentioned instability of the scheme, modified Galerkin Least Squares method is applied, cf. [7]. We start with the definition of the local element rezidual terms $\mathcal{R}_K^a$ and $\mathcal{R}_K^f$ defined on the element $K \in \mathcal{T}_h$ by

$$
\mathcal{R}_K^a(\tilde{\mathbf{w}}; \mathbf{v}, p) = \frac{3\mathbf{v}}{2\Delta t} - \nu \triangle \mathbf{v} + (\tilde{\mathbf{w}} \cdot \nabla)\,\mathbf{v} + \nabla p, \qquad \mathcal{R}_K^f(\hat{\mathbf{v}}^n, \hat{\mathbf{v}}^{n-1}) = \frac{4\hat{\mathbf{v}}^n - \hat{\mathbf{v}}^{n-1}}{2\Delta t}.
\tag{11}
$$

Further, the stabilizing terms are defined for $U^* = (\mathbf{v}^*, p^*)$, $U = (\mathbf{v}, p)$, $V = (\mathbf{z}, q)$ by

$$
\begin{aligned}
\mathcal{L}_{GLS}(U^*; U, V) &= \sum_{K \in \mathcal{T}_h} \delta_K \Big(\mathcal{R}_K^a(\tilde{\mathbf{w}}; \mathbf{v}, p), (\tilde{\mathbf{w}} \cdot \nabla)\,\mathbf{z} + \nabla q \Big)_K, \\
\mathcal{F}_{GLS}(V) &= \sum_{K \in \mathcal{T}_h} \delta_K \Big(\mathcal{R}_K^f(\hat{\mathbf{v}}_n, \hat{\mathbf{v}}_{n-1}), (\tilde{\mathbf{w}} \cdot \nabla)\,\mathbf{z} + \nabla q \Big)_K,
\end{aligned}
\tag{12}
$$

where the function $\widetilde{\mathbf{w}}$ stands for the transport velocity, i.e. $\widetilde{\mathbf{w}} = \mathbf{v}^* - \mathbf{w}_D^{n+1}$. The additional grad-div stabilization terms read

$$
\mathcal{P}_h(U, V) = \sum_{K \in \mathcal{T}_h} \tau_K (\nabla \cdot \mathbf{v}, \nabla \cdot \mathbf{z})_K.
$$

In the case of bounded convection velocity the choice of parameters according [7] for BB stable pair of FE (reduced scheme) would be possible. However, in order to obtain a fast and efficient multigrid method, the following choice of the parameters δ_K and τ_K is used

$$
\tau_K = \nu \left(1 + Re^{loc} + \frac{h_K^2}{\nu\,\Delta t} \right), \qquad \delta_K = \frac{h_K^2}{\tau_K},
$$

where the local Reynolds number Re^{loc} is defined as $Re^{loc} = \frac{h\|\mathbf{v}\|_K}{2\nu}$.

Problem 2 (Galerkin Least Squares stabilized approximations). *We define the discrete problem to find an approximate solution $U_h = (\mathbf{v}_h, p_h) \in \mathcal{W}_h \times \mathcal{Q}_h$ such that $\mathbf{v}_h$ satisfies approximately conditions (4a,b) and the identity*

$$a(U_h, V_h) + \mathcal{L}_{GLS}(U_h; U_h, V_h) + \mathcal{P}_h(U_h, V_h) = f(V_h) + \mathcal{F}_{GLS}(V_h), \tag{13}$$

for all $V_h = (\mathbf{z}_h, q_h) \in \mathcal{X}_h \times \mathcal{Q}_h$.

4. Multigrid solution of the linear system

The space-time discretized system (13) needs to be solved by some linearization scheme, e.g. by Oseen linearization procedure described e.g. in [18] or [19]. The solution of the linearized system (13) leads to the solution of a modified saddle point system

$$S\underline{\mathbf{v}} + B\underline{p} = \underline{f}, \qquad \tilde{B}^T \underline{\mathbf{v}} + \tilde{A}\underline{p} = 0, \tag{14}$$

where $\underline{\mathbf{v}}$ and $\underline{p}$ is the finite-dimensional representation of the finite element approximations of velocity and pressure, respectively. Let us mention that for the non-stabilized system (i.e. in the case of $\delta_K \equiv \tau_K \equiv 0$) we have $\tilde{A} = 0$ and $\tilde{B} = B$.

From the system of equations (14) the pressure degrees of freedoms can be formally eliminated by formally multiplying the first equation of (14) by $\tilde{B}^T S^{-1}$ from the left, i.e. we get the system of equations

$$\left(\tilde{B}^T S^{-1} B - \tilde{A} \right) \underline{p} = \tilde{B}^T S^{-1} \underline{f}, \tag{15}$$

or with notation $A_p = \tilde{B}^T S^{-1} B - \tilde{A}$ and $g = \tilde{B}^T S^{-1} \underline{f}$ we have

$$A_p \underline{p} = g,$$

which can be solved by the Richardson iterative method

$$\underline{p}^{(l+1)} = \underline{p}^{(l)} + C^{-1}(g - A_p \underline{p}^{(l)}), \tag{16}$$

where C is a suitable preconditioner, see e.g. [19]. Nevertheless the choice of the preconditioner C is complicated in the case of convection dominated flows and the convergence of the scheme (16) is in this case slow. Moreover the stabilizing terms also badly influences the convergence rates.

In many cases and for small number of unknowns, the system can be solved with the aid of a direct solver, which yields fast, efficient and robust scheme. We refer to direct solver UMFPACK, cf. [4], which in the cases studied by the authors up to now [18] was efficient for number of unknowns less then approximately 10^5. However, with further increase of the number of unknowns the memory and CPU requirements grows too fast, so that the fast and efficient solution becomes impossible. One possibility is to use the parallel implementation of multi-frontal method, cf. [1].

Here, the solution of the system (14) is carried out by a simplified version of multi-grid method. Only single mesh and two levels of solution (coarse and fine grid levels) are used. The fine grid is represented by the used higher order finite elements (here Taylor-Hood finite elements, i.e. P2/P1 approximations for velocity/pressure). The coarse grid is considered as lower order finite elements (i.e. equal order P1/P1 approximations for velocity/pressure). The solution on the coarse grid can be obtained with the aid of direct solver UMFPACK, which
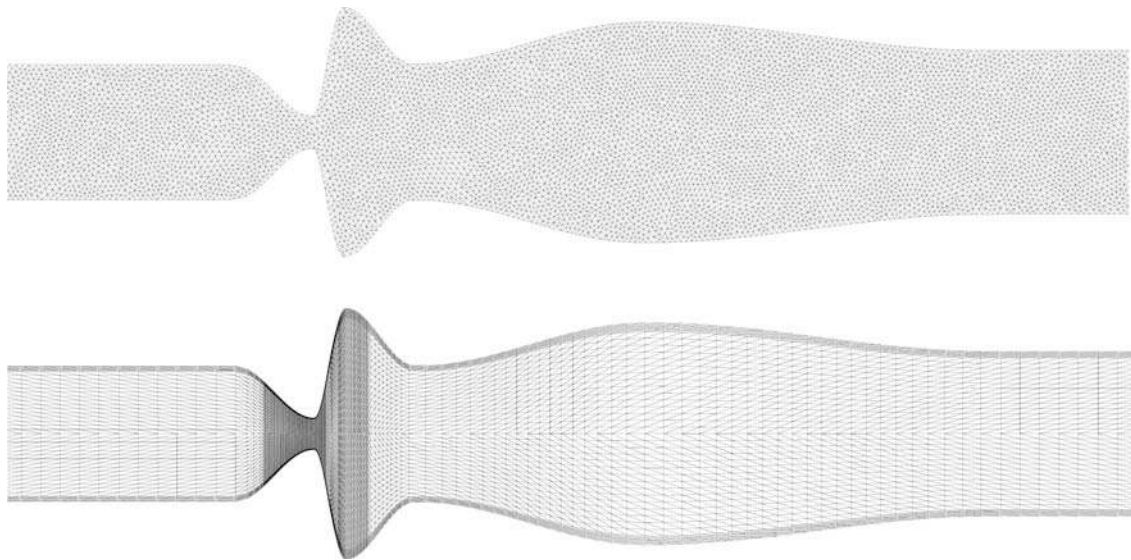
Fig. 2. The employed grids: the isotropic non-symmetric mesh (upper part) with 12 219 vertices and 23 709 elements and approximately 8×10^4 unknowns for flow problem, and the anisotropic axisymmetric mesh (lower part) with 8 241 vertices and 16 000 elements (resulting in 6×10^4 unknowns)

was found to be fast enough in the studied cases. On the fine grid the multiplicative Vanka-type smoother is used, cf. [9, 10]. This approach (i.e. the direct solver on coarse grid and Vanka-type smoother on fine grid) resulted in an efficient and fast method, which can be easily implemented. The performance of the multigrid method was found to be excellent for the isotropic grids. In the case of anisotropic mesh refinement, the convergence rates nevertheless become worse. The proper solution in this case is subject of a further study.

5. Numerical results

In this section the numerical results for air flow in a symmetric two-dimensional channel are presented. The channel geometry described in [14] is employed here, see also Fig. 1.

5.1. Stationary solution

First, we consider the non-moving computational domain Ω, where the influence of isotropically and anisotropically refined meshes is studied, see Fig. 2.

The following constants were used in the computations: fluid density $\rho_\infty = 1.225 \text{ kg m}^{-3}$ and kinematic viscosity $\nu = 1.5 \times 10^{-5}$ m²/s, the width of the inlet part of the channel is $H = 0.0176$ m, the total length of the channel $L = 0.16$ m, and the constant gap width $g \equiv 4.4$ mm.

The boundary condition (4d) in the presented computations is replaced by the condition (5), where the constant flow velocity is presribed $\mathbf{v}_D(x, t) = (U_\infty, 0)^T$ at the inlet part of boundary Γ_I, and U_∞ was chosen in the range 0.01–0.05 m s^{-1}. The numerical results for stationary solution and different Reynolds numbers ($Re = \frac{1}{8}LU_\infty/\nu$) are presented in Figs. 3–4, where the isolines of the magnitude of velocity are shown. The results computed on both meshes for same Reynolds numbers show that even for low Reynolds numbers several stationary symmetric and nonsymmetric solutions exist. Fig. 3 (left) shows the symmetric solution obtained on both meshes for $Re = 20$. For $Re = 40$ and $Re = 50$ in Figs. 3–4 on isotropic mesh
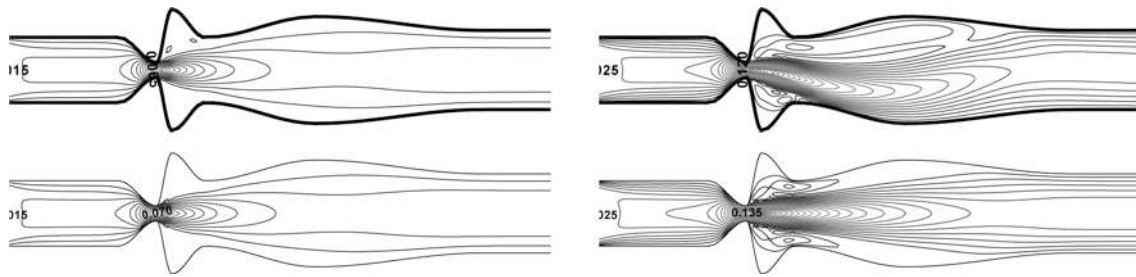
Fig. 3. The isolines of flow velocity magnitudes for Reynolds number 20 (left) and 40 (right) on isotropic mesh (upper part) and anisotropic mesh (lower part)
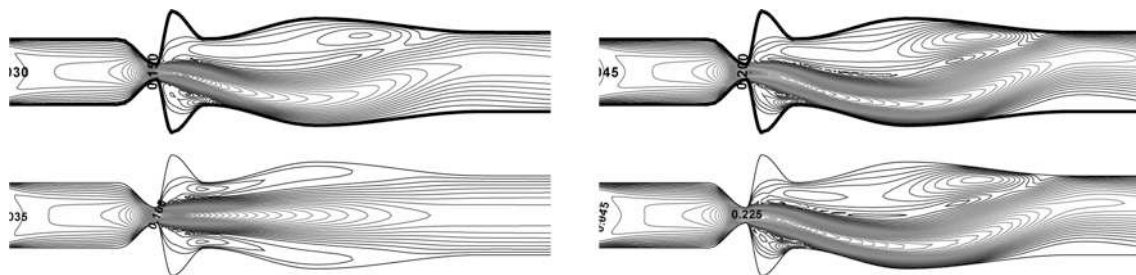

Fig. 4. The isolines of flow velocity magnitudes for Reynolds number 50 (left) and 70 (right) on isotropic mesh(upper part) and anisotropic mesh (lower part)

the non-symmetric solution was obtained, whereas on the anisotropical symmetric mesh the solution remains symmetric. For higher Reynolds number $Re > 50$ both solutions become non-symmetric.

5.2. Flow in channel with vibrating vocal folds

The numerical results for flow in vibrating channel are presented for physically relevant pressure drop, inlet flow velocity, frequency of vibrations and width of the channel, which leads to the Reynolds numbers in the range $Re = 1\,000 - 3\,000$.

The computations were carried out for the pressure drop of 400 Pa, i.e $p_{ref}^i = 400$ Pa and $p_{ref}^o = 0$ Pa. The initial condition was chosen as $\mathbf{v}^0 \equiv 0$ and the isotropically refined mesh was used, cf. Fig. 5. The gap oscillates harmonically around the mean gap value $\overline{g} = 4.4$ mm in the interval $g(t) \in [3.2\text{ mm}, 5.6\text{ mm}]$ with frequency $f = 100$ Hz .
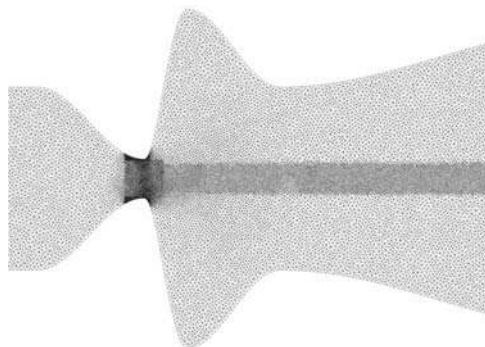

Fig. 5. The isotropic mesh used for multigrid solution of oscillating wall with 42 576 vertices and 84078 elements yielding approximately 4×10^5 unknowns for the flow problem
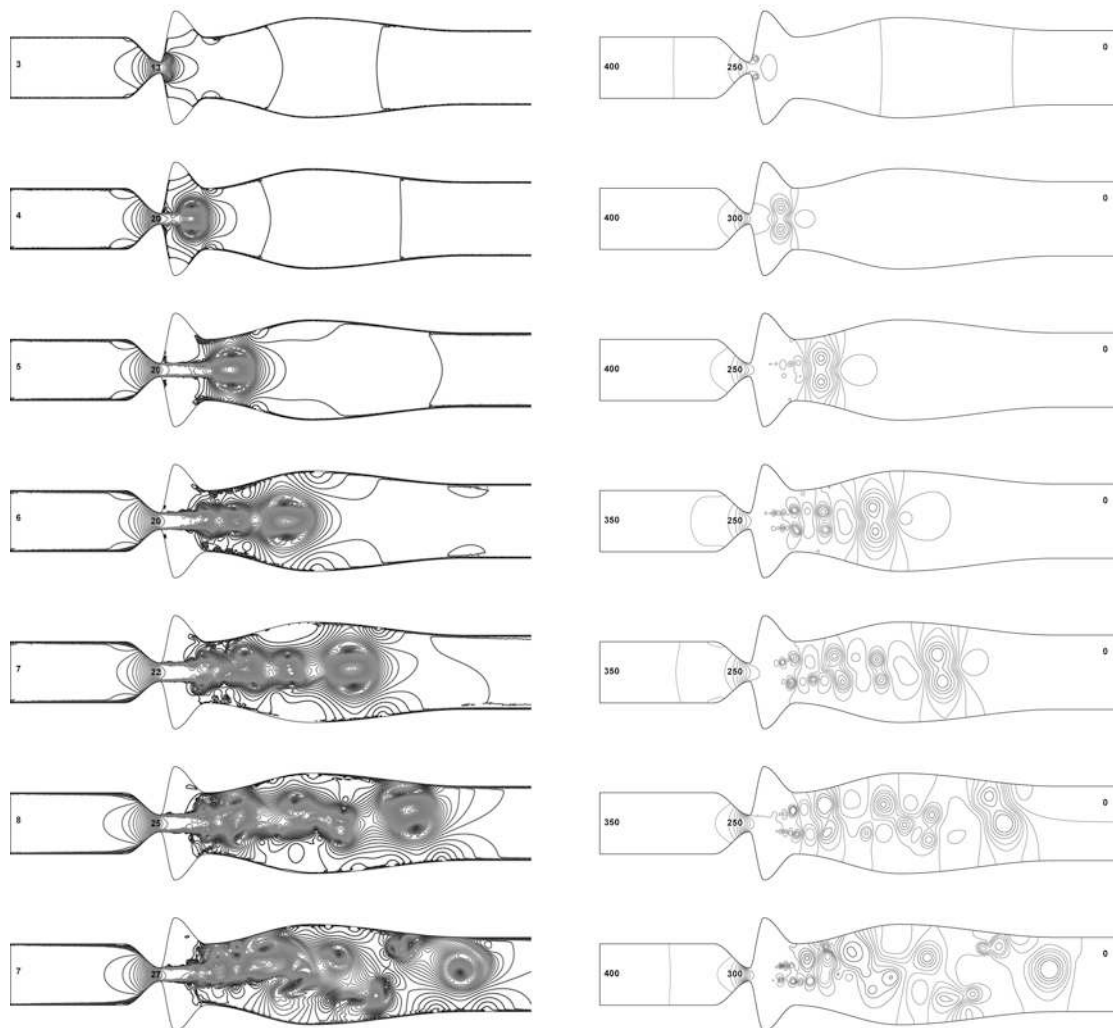
Fig. 6. The isolines of velocity magnitude (left) and pressure (right) in a sequence of time instance (from top to bottom, Part 1)

The results are shown in Figs. 6–7 for the time instants marked in Fig. 8. The sudden expansion in the modelled glottal region leads to the faster flow in the vibrating narrowest part of the computational domain and to complicated flow structures in the outlet part of the channel. Similar effects were observed experimentally in [15]. The inlet flow velocity and the flow velocity on the axis of symmetry at the narrowest part of the channel are shown in Fig. 8. The both values oscillates with a similar frequency as the prescribed motion of the wall. However, the graphs are noisy partially due to the complicated flow structures downstream.

6. Conclusion

The paper presents the developed mathematical method and applied numerical technique for solution of fluid-structure problems encountered in biomechanics of voice production. The method consists of the advanced stabilization of the finite element method applied considering the moving domain. In order to obtain fast solution of the discretized problem a simplified multigrid method was applied, which allowed solution of significantly larger system of equations compared to the previously used approach, see e.g. [18].
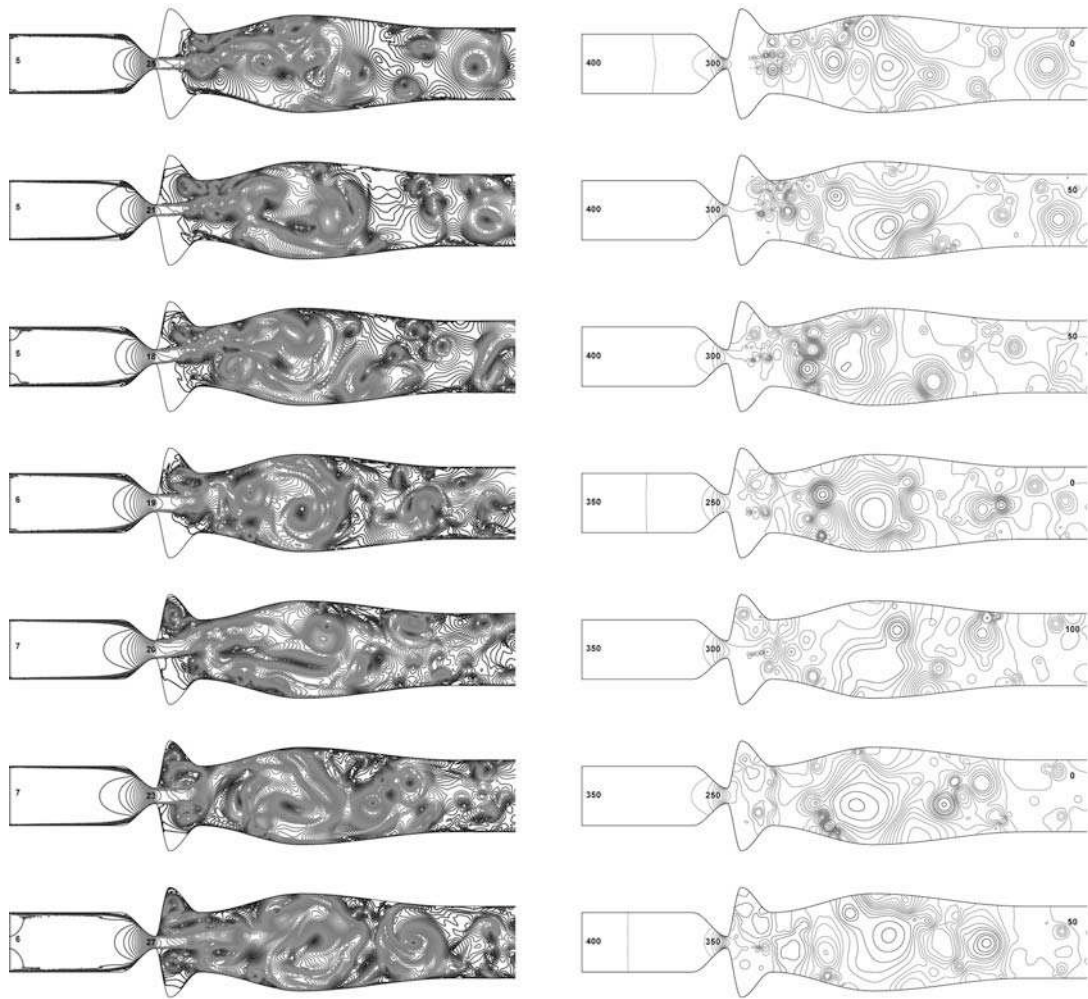
Fig. 7. The isolines of velocity magnitude (left) and pressure (right) in a sequence of time instance (from top to bottom, Part 2)
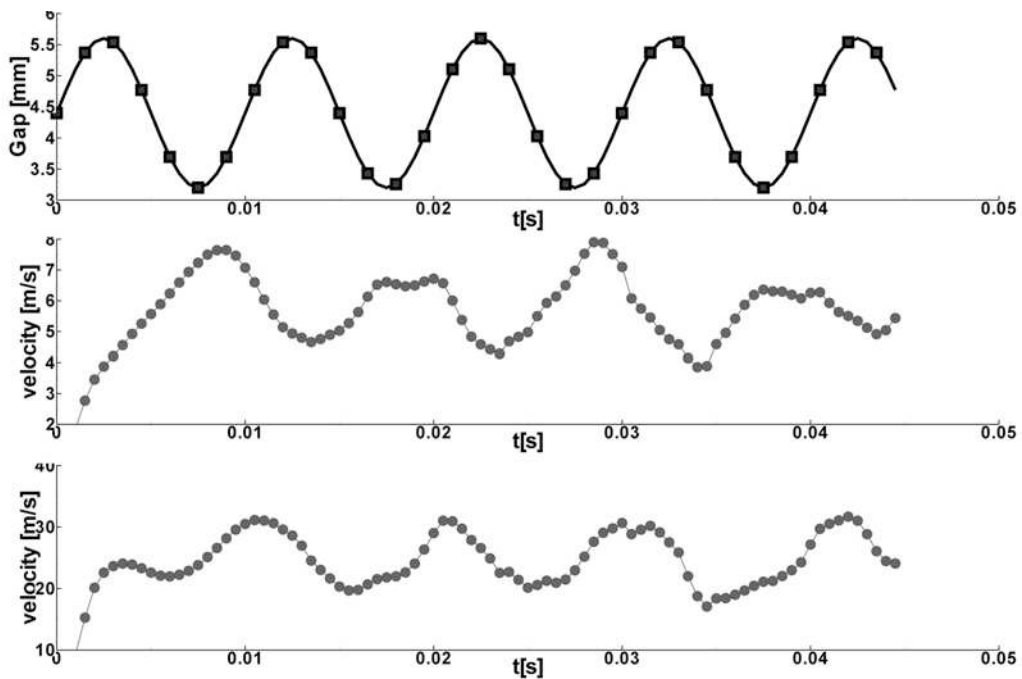

Fig. 8. The gap oscillations $g(t)$ (upper graph), the computed flow velocity at the inlet (middle), and the computed flow velocity in the glottal orifice (lower graph)

The influence of the isotropic and anisotropic meshes was studied and the multigrid technique was applied on a challenging problem of flow in symmetric channel with vibrating walls. The numerical results were presented showing the Coanda effect and complicated structure of small vortices and large size eddies generated at the glottal region by vibrating vocal fold. Similar vortex flow structures and Coanda effects were identified experimentally in [15].

Acknowledgements

References

[1] Amestoy, P. R., Guermouche, A., L'Excellent, J.-Y., Pralet, S., Hybrid scheduling for the parallel solution of linear systems. Parallel Computing, 32:136–156, 2006.

[2] Ciarlet, P. G., The Finite Element Methods for Elliptic Problems. North-Holland Publishing, 1979.

[3] Codina, R., Stabilization of incompressibility and convection through orthogonal sub-scales in finite element methods. Computational Method in Applied Mechanical Engineering, 190:1 579–1 599, 2000.

[4] Davis, T. A., Duff, I. S., A combined unifrontal/multifrontal method for unsymmetric sparse matrices. ACM Transactions on Mathematical Software, 25:1–19, 1999.

[5] Dolejší, V., Anisotropic mesh adaptation technique for viscous flow simulation. East-West Journal of Numerical Mathematics, 9:1–24, 2001.

[6] Feistauer, M., Mathematical Methods in Fluid Dynamics. Longman Scientific & Technical, Harlow, 1993.

[7] Gelhard, T., Lube, G., Olshanskii, M. A., Starcke, J.-H., Stabilized finite element schemes with LBB-stable elements for incompressible flows. Journal of Computational and Applied Mathematics, 177:243–267, 2005.

[8] Heywood, J. G., Rannacher, R., Turek, S., Artificial boundaries and flux and pressure conditions for the incompressible Navier-Stokes equations. Int. J. Numer. Math. Fluids, 22:325–352, 1992.

[9] John, V., Higher order finite element methods and multigrid solvers in a benchmark problem for the 3D Navier-Stokes equations. Int. J. Num. Meth. Fluids, 40:775–798, 2002.

[10] John, V., Tobiska, L., Numerical performance of smoothers in coupled multigrid methods for the parallel solution of the incompressible Navier-Stokes equations. Int. J. Num. Meth. Fluids 33, 33:453–473, 2000.

[11] Nobile, F., Numerical approximation of fluid-structure interaction problems with application to haemodynamics. PhD thesis, Ecole Polytechnique Federale de Lausanne, 2001.

[12] Nomura, T., Hughes, T. J. R., An arbitrary Lagrangian-Eulerian finite element method for interaction of fluid and a rigid body. Computer Methods in Applied Mechanics and Engineering, 95:115–138, 1992.

[13] Otto, F. C., Lube, G., Non-overlapping domain decomposition applied to incompressible flow problems. Contemporary Mathematics, 218:507–514, 1998.

[14] Punčochářová, P., Fürst, J., Kozel, K., Horáček, J., Numerical simulation of compressible flow with low mach number through oscillating glottis. In J. Horáček, I. Zolotarev, editor, Flow Induced Vibrations, Prague, 2008. Institute of Thermomechanics, CAS.

[15] Šidlof, P., Fluid-structure interaction in human vocal folds. PhD thesis, Charles University, Faculty of Mathematics and Physics, 2007.

[16] Sváček, P., Feistauer, M., Application of a Stabilized FEM to Problems of Aeroelasticity. In Numerical Mathematics and Advanced Application, pp. 796–805, Berlin, 2004. Springer.

[17] Sváček, P., Feistauer, M., Horáček, J., Numerical simulation of a flow induced airfoil vibrations. In Proceedings Flow Induced Vibrations, volume 2, pp. 57–62, Paris, 2004. Ecole Polytechnique.

[18] Sváček, P., Feistauer, M., Horáček, J., Numerical simulation of flow induced airfoil vibrations with large amplitudes. Journal of Fluids and Structure, 23(3):391–411, 2007.

[19] Turek, S., Efficient Solvers for Incompressible Flow Problems: An Algorithmic and Computational Approach. Springer, Berlin, 1999.

[20] Verfürth, R., Error estimates for mixed finite element approximation of the Stokes equations. R.A.I.R.O. Analyse numérique/Numerical analysis, 18:175–182, 1984.